Design and Flight Testing of an Integrated Solar Powered UAV and WSN for Greenhouse Gas Monitoring Emissions in Agricultural Farms*

Alexander Jairo Rojas Malaver *CPME*, Luis Felipe Gonzalez *ARCAA*, Nunzio Motta *CPME* and Tommaso Francesco Villa *CPME*, Victor Kwesi Etse *SEF*, Eduard Puig *ARCAA*

Abstract—**There is an increased interest in measuring the amount of greenhouse gases produced by farming practices . This paper describes an integrated solar powered Unmanned Air Vehicles (UAV) and Wireless Sensor Network (WSN) gas sensing system for greenhouse gas emissions in agricultural lands. The system uses a generic gas sensing system for CH4 and CO2 concentrations using metal oxide (MoX) and non-dispersive infrared sensors, and a new solar cell encapsulation method to power the unmanned aerial system (UAS)as well as a data management platform to store, analyze and share the information with operators and external users. The system was successfully field tested at ground and low altitudes, collecting, storing and transmitting data in real time to a central node for analysis and 3D mapping. The system can be used in a wide range of outdoor applications at a relatively low operational cost. In particular, agricultural environments are increasingly subject to emissions mitigation policies. Accurate measurements of CH4 and CO2 with its temporal and spatial variability can provide farm managers key information to plan agricultural practices. A video of the bench and flight test performed can be seen in the following link:**

https://www.youtube.com/watch?v=Bwas7stYIxQ.

I. Introduction

Agricultural greenhouse gas emissions can come from several sources; soil management, enteric fermentation, manure management as well as C02 from fossil fuel consumption, Agricultural soil management emissions for instance are nitrous oxide emissions which can account for about 55-65% of the total emissions from the agricultural sector. The large increase in the use of nitrogen fertilizer for the production of high nitrogen consuming crops like corn or wheat has increased the emissions of nitrous oxide. The use of nitrogen fertilizer is essential for profitable crop production. Some practices that use nitrogen fertilizer more efficiently have the potential to reduce nitrous oxide emissions while reducing production costs. Additionally reducing nitrogen fertilizer volumes reduces the risk of polluting ground waters. Methane is produced by ruminant animals such as cattle, goats and sheep during the digestive process as a result of a microbial fermentation. Beef cattle for example can account for about 70 percent and dairy cattle for about 25 percent of methane emissions. If beef and dairy cattle numbers increase, methane emissions will also increase [1].

Even though there are several methods used for measuring emissions in farms they have some limitations mainly in being restricted to be at a static location and cost of deploying several measuring stations around a farm also presents some changes in limited available power around a large broad acre farm [2].

This paper discusses the development, integration, and flight testing of a gas sensing system installed on a UAV and a WSN. This methodology represents a new opportunity to measure the spatial and temporal distribution of emissions. By monitoring the variability of agricultural emissions, farm managers can adapt agricultural practices to existing and future emissions mitigation policies. Figure 1 illustrates the concept developed.

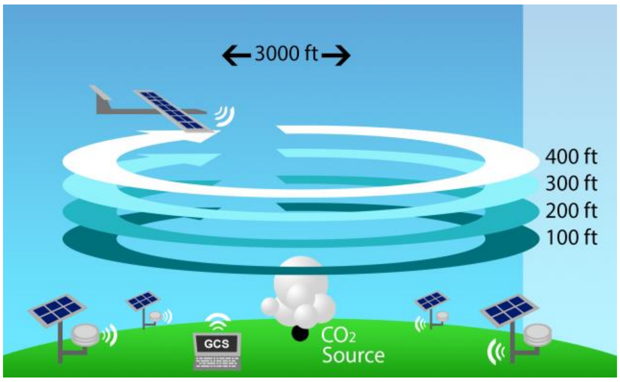

Figure 1 – Concept of a solar powered WSN and UAV gas sensing system.

UAVs have been used as an aerial remote sensing platform to measure environmental gases. UAV technologies are becoming a low cost but powerful tool to reach remote areas and survey relatively large regions [3,4]. In recent years, optical gas sensing devices have been widely integrated into UAV platforms. Watai et al.[5] for instance discussed a non-dispersive infrared (NDIR) sensing system to monitor atmospheric CO2 concentration onboard a small UAV, and designed an economic and accurate gas sensor system (± 0.26 ppm precision).The system performed several flight tests and achieved one hour flight autonomy with a 3.5 kg payload. McGonigle et al.[6] reported the first measurements of volcanic gases with a helicopter UAV at La Fossa crater, Volcano, Italy using an ultraviolet and infrared spectrometer to

* Queensland Government through the NIRAP project.
ARCAA for their technical support.

measure SO2 and CO2 gas concentrations. The UAV had 12 minutes of flight autonomy, carrying a 3 kg payload. Astuti et al.[7] developed a UAV for volcanic monitoring on Mt Etna using a fixed wing UAV to carry a CO2 infrared spectrometer and a SO2 electrochemical sensor. All these earlier research have achieved to autonomously sense gases using UAVs but the need to design and develop an efficient integrated system to continuously monitor and estimate gas concentrations has not been undertaken. Hence this paper is intended to tackle this issue by combining UAVs and WSN. The rest of the paper is organized as follows: section 2 discusses Solar Powered Wireless Sensor Network (WSN) Subsystem, section 4 describes the solar powered UAV, section 4 discuses WSN and UAV field tests, and section 5 presents conclusions and future work.

II. Solar Powered Wireless Sensors Network (WSN) Subsystem

Malaver et al described a generic gas sensing system and its application to WSN [8], developed as part of a collaborative research project between Brescia University (Italy) and QUT (Australia). We integrate a CO2 NDIR sensor also termed as the nano-sensor (CDM30K, Figaro Inc., Osaka, Japan), which is pre-calibrated from factory at 0 and 400 ppm, however the accuracy of the reading were cross checked with a LI-840A CO2 analyzer showing an overall error in the measurements of 5%. The signal output of the module is a DC voltage between 0 and 4 V, which represents 0–2000 ppm, respectively [9].

In This paper we extend the earlier work by adapting the gas sensor system to be installed on a Solar Powered UAV. The four principal components of the gas sensor system are shown in Figure 2: a network board, a gas sensor and sensor board interface, a humidity sensor, a heat sensor and control and solar panel and power electronics. The network card acquires the signal from the gas sensors and is able to propagate the data throughout multiple wireless sensor nodes in order to reach the base node. The base node communicates the data to the field computer, data of which can be stored, displayed and shared on a live webpage.

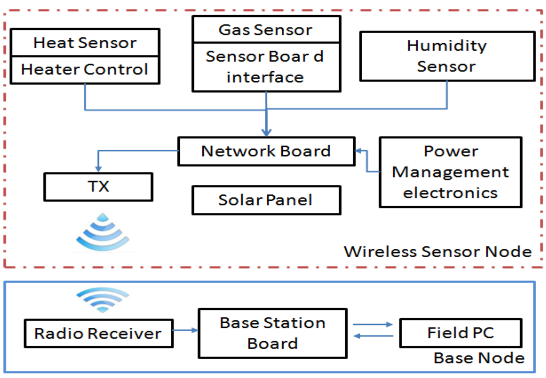

Figure 2 – Wireless gas sensing system node and base node configuration.

III. Solar Powered UAV

The UAV has three main sub-systems that are integrated with the airframe in order to estimate gas concentration, navigate, and keep powered during operations. These sub-systems are depicted in Figure 3.

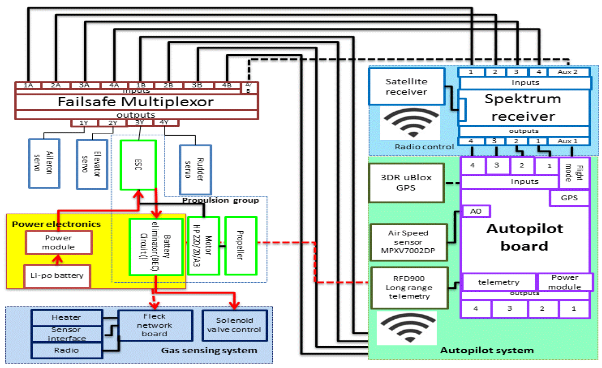

Figure 3 – General configuration of the UAV avionics integrated with the gas sensing system.

A. *Gas Sensing System*

The same gas sensing technology described in section 2 and used on the WSN was integrated to the UAV platform with some modifications in size, weight and power. Figure 4 illustrates these adaptations. The sample intake was adapted to allow the volume of gas volume for measurements.

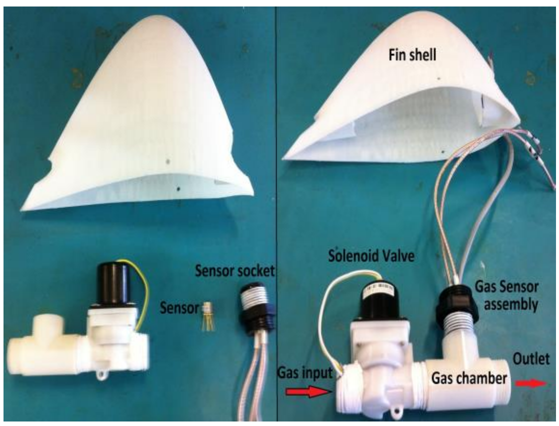

Figure 4 – Airborne gas sensing system: aerodynamic fin shell, gas sensor, sensor socket, gas chamber and solenoid valve.

The power for the gas sensing system is provided by an electronic battery eliminator circuit (BEC) that provides up to 5 VDC, 2 A. The 6 V required by the solenoid valve is provided by a step-up converter circuit attached to the BEC. Once the sensor board acquires the sensor signal, the information is transmitted to the base node using the radio module, antenna of which is installed on the top of the airframe.

B. UAV and Navigation System

The UAS developed in this work was based on the Green Falcon UAV[8,10]. The UAV airframe is easy to transport for fast deployment and hand launch. It has a wingspan of 2.52 *m*, AR of 13, and fuselage length of 960 *mm*.

The main component of the navigation system is the autopilot, which is equipped with an air speed sensor, gyro sensor, accelerometer, magnetometer, barometric pressure, GPS, airspeed and fail safe system. The principal goal of this device is to navigate the aircraft by controlling the altitude, speed, and direction. The autopilot used for the UAS was the ArduPilot Mega 2.5, which is a complete open source autopilot system with a high benefit/cost ratio and low weight (23 *g*). The autopilot system works mainly in three modes: (*i*) autonomous mode to fully perform unmanned mission by pre-programing waypoints from the ground control station (GCS); (*ii*) stabilised mode to assist a ground pilot in controlling and stabilising the flight of an aircraft where the pilot has partial control of the aircraft and when there is no pilot input the autopilot will maintain a level flight; (*iii*) and manual mode, which is useful to perform the pre-flight check as the autopilot acts as a pass-through for all RC commands and also allows the pilot to freely preform manual take-offs, manoeuvres and landings when the autopilot is not pre-programed to perform these tasks. In all modes, the autopilot is capable of transmitting relevant flight information such as roll, pitch, yaw, airspeed, GPS position and battery status to the GCS by using the telemetry module. The GPS system used was a LEA-6 (UBlox), which consumes low power, is small and lightweight (16.8 *g*) it has an update rate up to 5 *Hz* and is ideal for UAV applications. When the GPS is connected to the autopilot the coordinates are transmitted to the GCS using the same telemetry module of the autopilot. The GPS connects directly to the autopilot GPS port, and uses the RX, TX, GND and 5 *V* connections.

C. Power Management and Solar Wing

The total energy demand of the UAV was calculated based on the power consumption of the avionics, motor and gas sensing system, plus the lost energy caused by the efficiency of electronics and avionics (equation 1).

$$E_{demand\_total} = \frac{(E_{avionics} + E_{gas\_s})}{\eta_{power\ electronics} \times \eta_{avionics}} \quad \textbf{(1)}$$

Where the efficiency of the power electronics (η_{pe}) is 0.86, and the avionics (η_{av}) is 0.90.

Replacing values in Equation (1):

$$E_{demand_{total}} = \frac{(42.12\ Wh + 0.8\ Wh)}{0.86 \times 0.9}$$

$$E_{demand\_total} = 55.4\ Wh$$

The total energy demand (55.4 Wh) needs to be supplied by the solar wing and the battery. The solar wing was constructed using small silicon solar cell (SSC) ribbons connected in serial and parallel configuration to achieve the voltage and current required. Each SSC ribbon has an area of 0.00375 m^2 and an average of 12 *%* efficiency. The maximum area for the solar panels is limited by the wing area (490 cm^2), ailerons, narrow ends, and the area allocated for the gas sensor system (53 cm^2). Careful analysis of the location and configuration of the solar panels lead to 70 SSC ribbons were distributed along the three parts of the wing by placing 19 units on each side wing (total 38), and 32 units in the middle, for a total of 70 SSC units (0.2625 m^2). The weight density of a single SSC ribbon with the tabbing wire installed is 0.53 kg/m^2. A flexible capsule with the shape of the wing was made to allocate the SSC panels, to avoid losses in aerodynamic performance and to withstand mechanical stress due to in flight vibrations of the UAV. The solar panels were encapsulated using a clear resin, which is flexible and totally transparent to avoid output power losses. Figure 5 shows the UAV with the solar wing in flight.

The internal connections are in serial configuration to obtain the desired voltage of each panel. The side wing panels were connected in series to reach a V_{oc} of 19 *V*, which produced a current flow of 1.16 *A*. The middle wing panel is the main section, and consisted of 32 SSC ribbons in serial configuration to produce a V_{oc} of 16 *V*, and I_{sc} of 1.16 *A*. The right and the left wing panels in serial configuration were connected in parallel to the middle wing panel to produce a final V_{oc} and I_{sc} value between 16-19 *V*, 2 *A*, respectively.

Figure 5 – Green Falcon UAV in flight at Christmas Creek farm.

The total wing weight is 1610 g which means that 650 g is due to the SSC panel and encapsulation mass.

A commercial battery that complements the solar panel to meet the energy demand of the aircraft is a 4 cell, 3.0 Ah lithium polymer battery, which provides a nominal energy output of 44.4 Wh. However, for safety reasons and technical limitations, only 80 % of the battery capacity (35.52 Wh) was taken into account. The total energy available is therefore 59.14 Wh, which is enough energy to satisfy the demand of 55.4 Wh. The electronic board used to manage the solar and battery power is based on the BQ 24650 EVB from Texas Instruments [11]. The board works as a Maximum Power Point Tracker (MPPT), battery charger, and power path manager. This chip is from the same family as the nodes used for the WSN, with a battery charge/discharge efficiency of 86 %. The system is easy to setup, as the circuit board has only three ports; one for the solar power inlet, one for the lithium battery, and the output power to energise the UAV systems.

D. Some Propulsion System and Total Aircraft System

The main components of the propulsion group of the aircraft are the electronics speed controller (ESC); the brushless motor; and the propeller. The ESC used was the Plush 40 *A*, which can provide up to 40 *A* to the motor with a smooth throttle response, integrated battery eliminator circuit (BEC, 5*V*/3*A*), small size, weights 33 *g*, and is compatible with lithium polymer batteries with 2 to 6 *cells*.

The ESC regulates the power from the battery to run the avionics and gas sensing system simultaneously. In the case of an energy shortage, the ESC cuts the motor off and maintains a minimum power to allow the pilot manoeuver an emergency landing. The brushless motor used was the *Plettenberg* HP/220/20/A3 P6 SL 5:1.

The weight distribution of the UAS with the sensing system installed is illustrated in Figure 6 which shows the breakdown for the CO_2 system only, similar results were obtained for the nano-sensor system. The total weight of the UAS with the CO_2 system was 2573 *g*, and with the nano-sensor system 2615 *g*. It is clear from Figure 6 that the wing and fuselage were the heaviest parts in the UAV, while the CO_2 gas sensing system or the nano-sensor system represents only 12 *%* and 14 % of the total weight, respectively.

The power electronics had an average output voltage of 14.2 *V*, and the current intensity reached its maximum peak of about 6.5 *A* (consuming about 80 *W*), during take-off manoeuvres; however the average current consumption fluctuated between 1 *A* to 3 *A* (about 15 to 40 *W*), during regular flight operation.

According to the GCS, the energy consumption of the UAV during the flight operation was in average 25 *Wh*, which is lower than the average energy measured in the bench test of about 40 *Wh*. The possible reason for this lower consumption is that the throttle of the motor was more active during the bench test than in the real flight operation, which is a positive feedback for the final design of the solar powered UAV for continuous flight during sun-light hours.

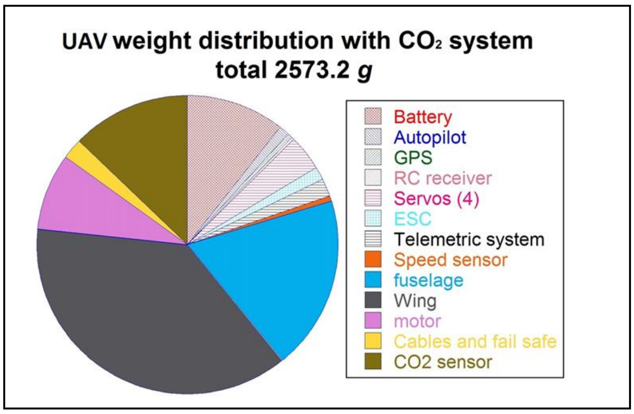

Figure 6 – Weight distribution of the Green Falcon UAV with CO2 gas sensing system.

IV. WSN AND UAV FIELD TEST

The target gas of the experiments was CO_2 measurements due to the availability of the gas in the field testing area and the possibility of creating a contaminant source. Testing NO_2 and CH_4 in the field requires a different scenario that will be considered in future work. The WSN was calibrated and tested at Samford Ecological Research Facility (SERF) [8] however nly two of the four nodes developed for the WSN were tested in conjunction with the UAV as a proof of concept.

The complete system was tested at Christmas Creek, QLD, 23th July, 2013. The base station was located at the beginning of the airstrip, the pollutant source was located 30 *m* from the GCS, the CO_2 ground node and the weather station was deployed 20 *m* from the GCS, all south of the base node. The UAV mission was to fly in a circular trajectory up to an altitude of 50 *m* above ground level over the area monitored, above the sensor node and pollutant source. The CO_2 was released for 6 *min* at 0.0027 *kg/s* rate and average wind speed of 1.09 *m/s.*

CO_2 concentration values taken from ground and aerial nodes during the experiments are plotted in figure 7. The average CO_2 concentration registered by the ground node was 404 *ppm* during the first 164 *s*. Then, the average concentration increased slightly until it reached a peak of 442 *ppm* at the end of the experiment. The average CO_2 concentration registered by the aerial node was 400 *ppm*, with few CO_2 peaks above the average. The volume monitored by the UAV was 0.0012 km^3, based on the circular area travelled and flight altitude (~50 *m* AGL). The horizontal sampling resolution of the UAV was 88 *m/s* as the average cruise speed was 12.6 *m/s* and sampling frequency 7*s*. Vertical resolution of the samples was 10 *m* based on the uncertainty of the GPS and autopilot navigation. Figure 8 shows the UAV tracks during the experiment, the contaminant source origin and direction of the dispersion due to wind effect. The average wind speed was 1.5 *m/s*, mostly in North-east direction.

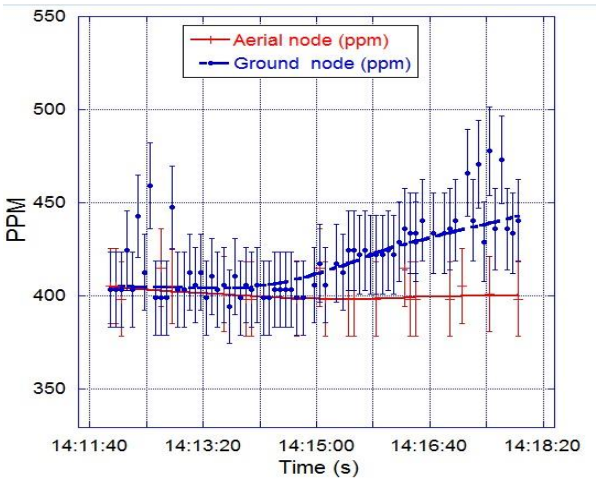

Figure 7 – CO2 readings from the ground and aerial nodes during the experiment at Christmas Creek, QLD, Australia in 23/07/2013.

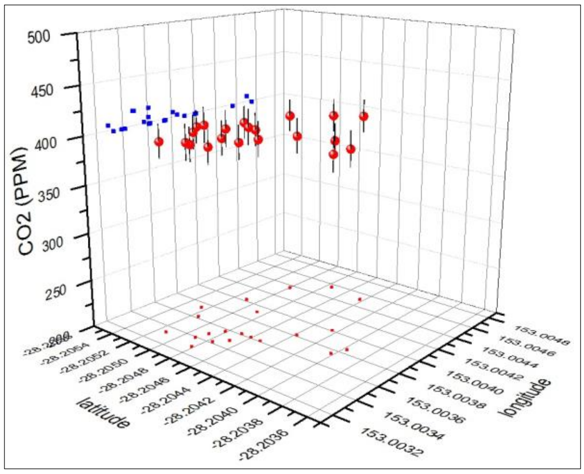

Figure 9 – Readings of the CO2 gas sensing system on board Green Falcon UAV, showing the latitude, longitude and concentration of each sample.

Figure 8 – GPS tracks of the UAV during the mission, the source of contamination and the wind direction.

Figure 9 shows the latitude and longitude coordinates of each sample with its respective CO_2 concentration. The fact that the CO_2 readings from the UAV did not show significant variations indicates that the contaminant release rate and duration were not long enough to affect significantly a volume of 0.0012 km^3 within the time span of the experiment (6 *min*). In addition, the wind strength diluted the pollutant emissions to levels below the sensitivity of the equipment. Geo-location of each sample was achieved by synchronising the logs of the network board and autopilot before the mission started. The ability to geo-locate the sample and register the time allows the reconstruction of the samples in three dimensions and facilitates the visualisation of local concentrations, analysis of their dynamics and correlations with variables such as temperature and pressure.

V. Conclusion

This paper described a generic gas sensing and monitoring system of a solar powered WSN and UAV for environmental monitoring. The solar powered UAV was assembled, equipped with the gas sensing system, and successfully tested in the field. It is recommended for further experiments to increase the contaminant rate release and duration to produce significant CO_2 variation in the volume monitored by the UAV. Faster sampling frequency is also desirable, especially when the wind blows in a specific direction, which narrows the detection area.

A video of the extensive bench test performed for this work on the Green Falcon UAV can be seen in the following link https://www.youtube.com/watch?v=Bwas7stYIxQ.

VI. Acknowledgment

The authors would like to acknowledge the financial support from the Queensland Government through the NIRAP project, “Solar powered Nano sensors”, ARCAA for their technical support, Fazl Alabodi and Mandeep Saini as well as the support from Steven Bulmer the Green Falcon pilot.

References

[1] Takle, Eugene, Hofstrand D., "Global Warming - Agriculture’s Impact on Greenhouse Gas Emissions." *http://www.extension.iastate.edu/agdm/homepage.html*. Iowa State University: University Extension, 20 Apr. 2008. Web. 7 June 2015.

[2] Jaichandran, R., and A. Anthony Irudhayarj. "Prototype system for monitoring and computing greenhouse gases." Carbon 1998 2005.

[3] Hung, J. Y. and Gonzalez, L. F. On parallel hybrid-electric propulsion system for unmanned aerial vehicles. *Progress in Aerospace Sciences*, *51*, pp. 1-17, 2012.

[4] Gonzalez, F., Castro, M. P. G.,Narayan, P., Walker, R., & Zeller,L. (2011). *Development of an autonomous unmannedaerial system to collect time-stamped samples from theatmosphere and localize potential pathogen sources*. Journal of Field Robotics, 28(6), 961–976.

[5] Watai, T. Machida, T. Ishizaki, N. Inoue, G. *A Lightweight Observation System for Atmospheric Carbon Dioxide Concentration Using a Small Unmanned Aerial Vehicle.* Journal of Atmospheric and Oceanic Technology, 23(5): p. 700-710, 2005.

[6] McGonigle, A. J. S. Giudice, G. Tamburello, A. Hodson, J. Gurrieri, S. *Unmanned aerial vehicle measurements of volcanic carbon dioxide fluxes.* Geophysical Research Letters, 35(6), 2008.

[7] Astuti, G. Longo, D. Melita, C.D. Muscato, G. Orlando, A. *HIL tuning of UAV for exploration of risky environments.* International Journal of Advanced Robotic Systems, 5(4): p. 419-424, 2008.

[8] Malaver Rojas, J.A. Motta, N. Gonzalez, L. F. Corke, P. Depari, A. *Towards the development of a gas sensor system for monitoring pollutant gases in the low troposphere using small unmanned aerial vehicles.* Workshop on Robotics for Environmental Monitoring, 2012.

[9] FIGARO. CDM30K Carbon Dioxide Sensor Module. Available online: http://www.figaro.co.jp/ en/topic/2012/01/announcement-of-co2-gas-sensor-module-cdm30k.html (accessed on 9 September 2014)

[10] Malaver Rojas, J.A. Motta, N. Corke, P. Bell, J. *Development of a gas nanosensor node powered by solar cells*. In *Solar2011, the 49th AuSES Annual Conference*, Australian Solar Energy Society, 2011.

[11] *bq24650EVM Synchronous, Switch-Mode, Battery Charge Controller for Solar Power*, T. Instrument, Editor. 2010.